GPS-FREE TERRAIN-BASED VEHICLE TRACKING PERFORMANCE AS A FUNCTION OF INERTIAL SENSOR CHARACTERISTICS

Kshitij Jerath and Sean N. Brennan
Department of Mechanical and Nuclear Engineering
The Pennsylvania State University
University Park, PA 16802
(kjerath@psu.edu, sbrennan@psu.edu)

ABSTRACT

Prior experiments have confirmed that specific terrain-based localization algorithms, designed to work in GPS-free or degraded-GPS environments, achieve vehicle tracking with tactical-grade inertial sensors. However, the vehicle tracking performance of these algorithms using low-cost inertial sensors with inferior specifications has not been verified. The included work identifies, through simulations, the effect of inertial sensor characteristics on vehicle tracking accuracy when using a specific terrain-based tracking algorithm based on Unscented Kalman Filters. Results indicate that vehicle tracking is achievable even when low-cost inertial sensors with inferior specifications are used. However, the precision of vehicle tracking decreases approximately linearly as bias instability and angle random walk coefficients increase. The results also indicate that as sensor cost increases, the variance in vehicle tracking error asymptotically tends to zero. Put simply, as desired precision increases, increasingly larger and quantifiable investment is required to attain an improvement in vehicle tracking precision.

INTRODUCTION

Several safety-critical and mission-critical applications [1], such as path planning, navigation and collision avoidance, require the ability to accurately and inexpensively localize and track the position of a vehicle. While the Global Positioning System (GPS) has placed itself as a viable contender for being the default system used to perform localization and tracking, it has many shortcomings that cannot be ignored, especially in safety-critical and mission-critical scenarios. Specifically, poor GPS signal reception, the ability to jam GPS signals and the requirement to maintain redundancy in vehicle automation and driver assist systems necessitates the development of other localization and tracking techniques [2]. These factors, along with the miniaturization and cost reduction of inertial sensors, have resulted in the growth of inertial navigation technology. This paper considers one of the promising alternatives to GPS, hereafter called *terrain-based localization*, which utilizes only terrain information such as attitude (pitch, roll and yaw) or features generated thereof, to localize and track vehicles [3] [4]. Put simply, terrain-based localization works by comparing the current attitude measurement against a database of previously recorded terrain attitude maps. The algorithm then utilizes a filtering scheme, such as particle filtering or Kalman filtering, to localize and track the vehicle through continuous correlation of incoming sensor measurements to the terrain database.

Today, a wide range of options exist for the system engineer trying to identify the appropriate sensor for a desired application. With regards to terrain attitude measurements in ground vehicles, several sensing techniques exist, which utilize LIDAR [5] [6], cameras [7] [8] or inertial sensors [9]. Typically, though, inertial sensors are used for attitude measurements in ground vehicles due to their ease of use, robustness and ruggedness. Within the category of inertial sensors too, there exist various options, separated by several orders of magnitude in terms of cost and precision [10]. With the development of micro electro-mechanical systems (MEMS) devices, inertial sensors have found applications in fields ranging from automotive safety and navigation to virtual reality and motion-based video games [11]. MEMS inertial sensors are typically low-cost, small-sized, designed for large volume production and lie at the lower end of the accuracy scale [10]. On the other hand, the development of optics-based inertial sensors, such as ring laser gyros and interferometric fiber optic gyroscopes (IFOG), has led to remarkable improvement in the quality of inertial measurements. However, optics-based inertial sensors are typically expensive and lie at the higher end of the accuracy scale. The choice and accuracy of inertial sensors plays a major role in the ability of the terrain-based localization

algorithm to provide an accurate estimate of the vehicle's position.

The accuracy of a sensor is usually characterized by quantifying the various individual noise sources that contribute to sensor measurement error, such as white noise, bias etc. [12] [13]. For example, for inertial sensors, manufacturers usually specify angle random walk, in-run bias instability, over-temperature bias instability, resolution, bandwidth etc. to characterize the constituent gyroscopes and accelerometers. Prior research indicates that fusing low-cost inertial sensors with GPS can provide accurate estimates of vehicle states [14] [15]. However, in the present context where only terrain information is available, such a correction is not possible. Thus, for the applications discussed above, it becomes necessary to identify how inertial sensor characteristics affect the localization accuracy of the algorithm. Further, the adoption of terrain-based localization methods requires that the system engineer know how to translate the application requirements, such as desired vehicle tracking accuracy, into the correct sensor specifications, in order to select the appropriate inertial sensor for the application.

In this paper, the effects of inertial sensor characteristics on vehicle localization accuracy, given a specific algorithm and environment, will be discussed. The given algorithm is a terrain-based localization algorithm that utilizes an Unscented Kalman Filter for performing vehicle tracking [16], and the given environment is the test track facility at the Larson Transportation Institute at the Pennsylvania State University. Thus, the paper attempts to elucidate a relationship between sensor characteristics and localization accuracy and in the process show that low-cost MEMS inertial sensors are indeed a viable option for terrain-based vehicle tracking. The remainder of this paper is organized as follows. Section 2 discusses the sensor modeling, characterization and simulation procedures. Section 3 includes a simulation-based analysis of the effects of sensor characteristics on vehicle tracking accuracy. Section 4 compares existing inertial sensors available on the market in terms of their ability to track a vehicle using the terrain-based localization algorithm. Section 5 concludes the paper with an overview of important results.

SENSOR MODELING, CHARACTERIZATION AND SIMULATION

This section discusses the various noise sources in inertial sensor measurements. It also details the procedure for identifying inertial sensor characteristics through Allan variance analysis and simulating a signal emanating from an inertial sensor with known characteristics. It is assumed that the measurements obtained from a sensor are corrupted by a variety of noise sources inherent to the sensor. For example, random flickering in the sensor's electronic components can cause bias drift or bias instability in inertial sensors [16]. The measurement error caused by these noise sources can be approximated by developing *noise models* for each source. *Noise modeling* is the process of specifying a functional form and a set of parameter values that represent a noise source. For example, bias instability is modeled as a first-order Gauss-Markov process [12]. On the other hand, s*ensor characterization* is the process of identifying and quantifying the model parameter values of the noise sources that contribute to sensor measurement error, using actual measurements collected from a sensor. In the included work, sensor characterization is performed using Allan variance and autocorrelation analyses due to the ease of error source identification they offer [13]. *Sensor simulation* is the process of using the known noise models to corrupt true values of the sensed variable in order to simulate 'noisy' sensor measurements. In the following subsections, aspects of sensor modeling, characterization and simulation will be discussed.

Noise Sources and Modeling

The primary noise sources that contribute to measurement error in inertial sensors are angle random walk (η) and bias instability (b) [14]. The noisy sensor measurements are calculated by adding the errors due to various noise sources to the true value, as shown in Eq. (1) :

$$\omega = \omega_{TRUE} + \eta + b \tag{1}$$

Angle random walk is modeled as a white noise applied to the angular rate measured by the gyroscope. Integration of the corrupted angular rate yields a random walk error in the angle (attitude) measurements, giving the noise source its name. The parameter used to specify angle random walk is the angle random walk coefficient (N) which is the square root of the noise power [17],

$$E[\eta^2] = N^2 \tag{2}$$

Bias instability is the result of the random flickering in electronic components and is modeled as a first-order Gauss-Markov process representing exponentially correlated noise, as shown in Eq. (3):

$$\dot{b} = -\beta b + \eta_b \tag{3}$$

where, $\beta = 1/T_c$, is the inverse of the correlation time, and η_b is white noise with $E[\eta_b^2] = \sigma_B^2 \approx (\beta^2 + \omega_0^2)\, B^2/\omega_0$, where B is the bias instability coefficient used to specify the noise, and ω_0 corresponds to the flicker noise cutoff frequency [16] [17]. Thus, given the noise parameters, measurements from a noisy sensor can be simulated using the discussed noise model. As mentioned before, the noise parameters for inertial sensors are determined using Allan variance analysis. This analysis procedure is discussed in the following subsection.

Allan Variance Analysis

The basic premise of Allan variance analysis is that the different noise sources that contribute to sensor measurement error have different power spectral densities, and their individual contributions can be quantified by observing the Allan variance in the corresponding time domain. Allan variance in the context of inertial sensors is defined as follows [16] [18]:

$$\sigma^2(\tau) = \frac{1}{2}\langle(\bar{\Omega}_{k+m} - \bar{\Omega}_k)^2\rangle \quad (4)$$

where $\bar{\Omega}_{k+m}$ represents the gyroscope mean angular rate in the k^{th} interval containing m measurements, τ denotes the correlation time and $\langle\cdot\rangle$ represents the ensemble average. The typical plots describing Allan variance for angle random walk and bias instability noise sources, as a function of correlation time, are included as Figure 1 and Figure 2, respectively. The parameters defining these noise models are obtained from the following expressions which bound their values, as detailed in [13]:

$$N = \frac{\sigma_A(\tau_N)\sqrt{\tau_N}}{60} \quad (5)$$

$$B = 0.6648\sigma_A(\tau_B) \quad (6)$$

where τ_N corresponds to the correlation time when analyzing the Allan variance graph for angle random walk, $\sigma_A(\tau_N)$ corresponds to the Allan deviation when the correlation time is τ_N, $\sigma_A(\tau_B)$ corresponds to the Allan deviation when the correlation time is τ_B, N is referred to as the angle random walk coefficient and B is referred to as the bias instability coefficient. The other parameter in the bias instability model, the correlation time T_C, is typically determined using experimental autocorrelation analysis, as discussed in [19].

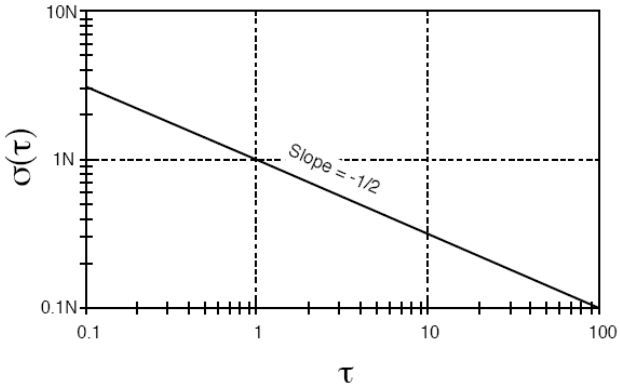

FIGURE 1: ALLAN DEVIATION PLOT FOR ANGLE RANDOM WALK [16]

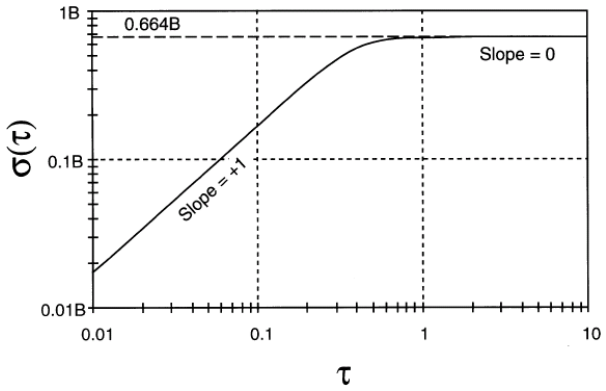

FIGURE 2: ALLAN DEVIATION PLOT FOR BIAS INSTABILITY [16]

Sensor Simulation and Validation of Noise Models

Armed with the knowledge of the angle random walk coefficient (N), the bias instability coefficient (B) and an estimate of the correlation time (T_C), the noise model for an inertial sensor can be generated. The noise model can then be used to corrupt true attitude data in order to obtain the 'noisy' attitude measurements from a simulated sensor. A sensor with pre-specified noise parameters is simulated in Simulink at a 100 Hz sampling rate, to obtain the noisy attitude measurements. While not the focus of this study, it is expected that changing the sampling rate will also have an effect on the sensor performance. Initial simulations were performed using typical sensor characteristics based on data provided in inertial sensor datasheets. The sensor characteristics, or noise model parameters, were selected to represent tactical-grade sensors on one end of the accuracy scale, and MEMS inertial sensors on the other. Figure 3 and Figure 4 compare the true attitude with the attitude measurements output by the simulated sensors using manufacturer-supplied noise values [21] [22].

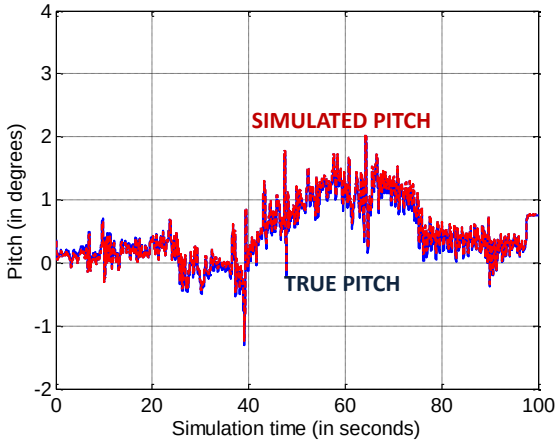

FIGURE 3: SIMULATED TACTICAL-GRADE INERTIAL SENSOR OUTPUT COMPARED TO TRUE ATTITUDE DATA. (N = 0.001 º/√SEC, B = 0.0001 º/SEC)

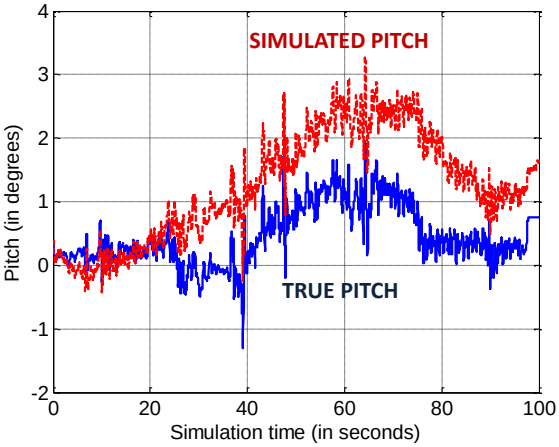

FIGURE 4: SIMULATED MEMS INERTIAL SENSOR OUTPUT COMPARED TO TRUE ATTITUDE DATA. (N = 0.01 º/√SEC, B = 0.01 º/SEC)

It may be observed that despite the noise, the simulated sensor outputs tend to match the "features" or "patterns" in the true attitude data. Further, the plots seem to agree with intuition that MEMS inertial sensors provide noisier measurements as compared to tactical-grade inertial sensors. This provides a qualitative confirmation of the validity of the noise models.

To fully validate the sensor noise model, the sensor characterization process is employed on the simulated sensor data. The noise model is validated by performing an Allan variance analysis as well as autocorrelation analysis to recover the noise parameters. The known and the recovered noise parameters are included in Table 1, whereas the Allan variance plot for the simulated sensor is included in Figure 5, and the autocorrelation plot is included in Figure 6. It is observed that the noise parameters recovered from the analysis of the simulated sensor data are in reasonable agreement with the pre-specified noise parameters provided as input to the noise model. Thus, the noise modeling scheme and simulated sensor data generation are consistent. The attitude measurements from a simulated sensor can now be fed to the terrain-based localization algorithm and the resulting vehicle tracking accuracy can be analyzed.

TABLE 1: INPUT AND RECOVERED NOISE PARAMETERS

Parameter	Input	Recovered
Angle random walk coefficient, N $(°/\sqrt{sec})$	0.0040	0.0041
Bias instability coefficient, B $(°/sec)$	0.005	0.0047
Correlation time, T_C (sec)	200	190.74

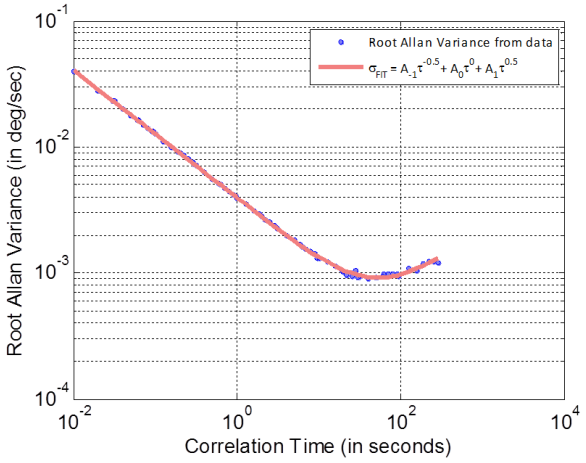

FIGURE 5: ROOT ALLAN VARIANCE PLOT FOR SIMULATED SENSOR DATA

EFFECTS OF INERTIAL SENSOR CHARACTERISTICS ON VEHICLE TRACKING ACCURACY

As the ability to simulate sensor data with known sensor characteristics has been introduced, the issue of the effects of these characteristics on the accuracy of vehicle tracking can be examined. As mentioned earlier, vehicle tracking is performed using a terrain-based tracking algorithm which utilizes an Unscented Kalman Filter. At this point, a brief overview of the vehicle tracking algorithm is in order.

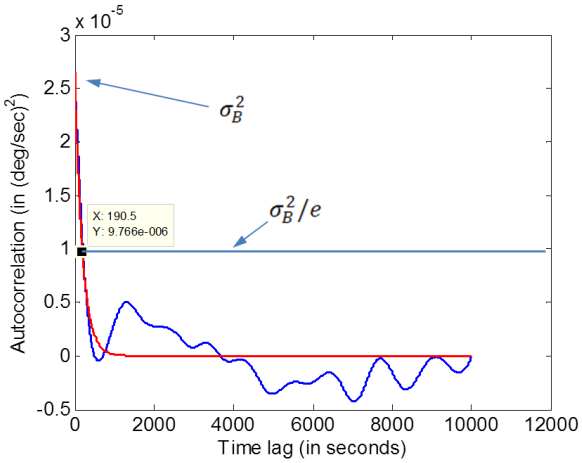

FIGURE 6: AUTOCORRELATION ANALYSIS FOR SIMULATED SENSOR DATA

Terrain-based Vehicle Tracking Using Unscented Kalman Filters

The basic premise of a terrain-based localization algorithm is that, as a vehicle travels over a road, an inertial measurement unit can be used to sense the terrain attitude (roll, pitch and/or yaw). The measured attitude can then be compared against a pre-recorded database or lookup table that contains attitude measurements along with the position coordinates of the entire road network. All locations on the road where the attitude matches the currently observed attitude are potential current positions for the vehicle. However, for tracking purposes, an estimate of the current location is usually known. Consequently, an Unscented Kalman Filter (UKF) can be used to update the current position estimate of the vehicle, as discussed in [20]. As the vehicle progresses and new measurements are obtained, the current position estimate of the vehicle is updated to continue to track the vehicle on the road network. For the purposes of this algorithm, the current position is defined as the distance of the vehicle from the last-visited intersection, and the tracking error is defined as the difference between the true and estimated positions.

While previous experiments indicate that terrain-based vehicle tracking is indeed a viable option, these experiments have primarily been performed using tactical-grade inertial measurement units [20]. Tactical-grade inertial sensors are designed to have a high degree of accuracy and their specifications indicate that they have lower angle random walk coefficients and bias instability coefficients as compared to MEMS-based inertial sensors. Table 2 lists the sensor characteristics of the Honeywell HG1700 [22], which is a tactical-grade sensor and utilizes a ring laser gyroscope, and the Analog Devices ADIS16367 [21], which is a MEMS inertial

sensor. Vehicle tracking accuracy has been examined for various simulated sensors whose sensor characteristics lie roughly in the range described by these two sensors. It must be noted at this point that the vehicle tracking algorithm does not estimate the bias in the sensor, i.e. sensor bias has not been chosen as a state in the state vector. The primary reason for doing so is that the stability of the Kalman filter cannot be guaranteed if bias correction is included without knowledge of the ground truth. As a preliminary example to indicate the qualitative differences in vehicle tracking accuracy, simulations were performed using sensors at the extreme ends of the sensor specification scale. Figure 7 includes the tracking error plots for the two simulated sensors with mentioned sensor characteristics. The simulated MEMS sensor has the following characteristics: $N = 0.01°/\sqrt{sec}, B = 0.01°/sec$. On the other hand, the simulated tactical-grade sensor has the following characteristics:$N = 0.001°/\sqrt{sec}, B = 0.0001°/sec$. As an immediate observation, it can be seen that even a simulated MEMS sensor is able to maintain vehicle tracking albeit at slightly larger tracking error values. This observation implies that the terrain-based localization algorithm has the potential to track vehicles even with low-cost sensors with inferior specifications. Next, the effects of varying angle random walk coefficients and bias instability coefficients on vehicle tracking error are analyzed. The values of the noise coefficients are chosen so as to span the range between the low-cost MEMS sensor and the tactical-grade sensor specifications.

TABLE 2: SENSOR CHARACTERISITICS [21] [22]

Parameter	Honeywell HG1700	Analog Devices ADIS16367
Angle random walk coefficient N $(°/\sqrt{sec})$	0.0016	0.033
Bias instability coefficient, B $(°/sec)$	0.0003	0.013

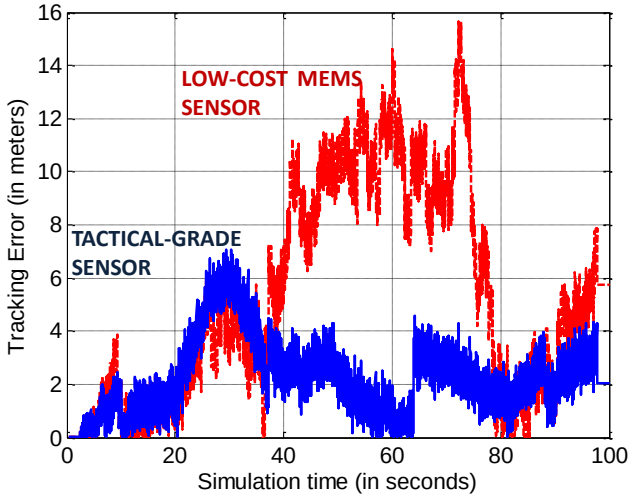

FIGURE 7: TRACKING ERROR WITH DIFFERENT SIMULATED SENSORS

Effects of Angle Random Walk on Vehicle Tracking Accuracy and Precision

Figure 8 depicts the plot of vehicle tracking accuracy using the terrain-based tracking algorithm as the angle random walk coefficient is varied from $0.001°/\sqrt{sec}$ to $0.01°/\sqrt{sec}$. Each data point on the thin lines indicates a set of simulations run with a fixed noise model. The thin lines in Figure 8 indicate the mean tracking error as the angle random walk coefficient is varied and the bias instability coefficient is held fixed at various values viz. B = 0.0001, 0.002, 0.004, 0.006, 0.008, and $0.01°/s$. The plot indicates that the mean tracking error increases as the angle random walk is increased from the minimum to the maximum value under consideration. The thick line in Figure 8 is the average of the mean tracking error across all bias instability coefficients. It has been included as a means to emphasize the following qualitative relationship: the mean tracking error increases as angle random walk coefficient increases. Within the range under consideration, this relationship may loosely be described as being quadratic in nature.

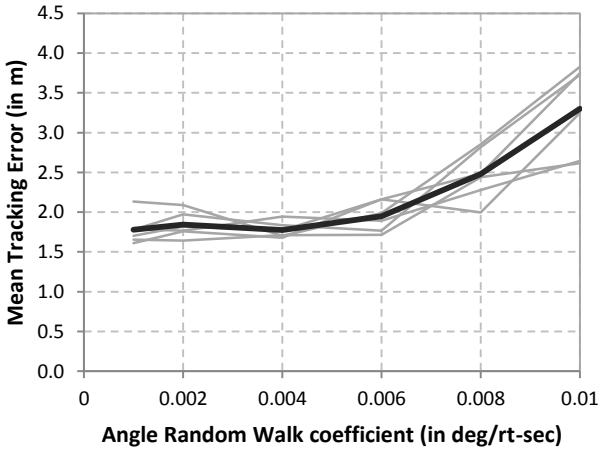

FIGURE 8: MEAN TRACKING ERROR FOR VARYING ANGLE RANDOM WALK COEFFICIENTS

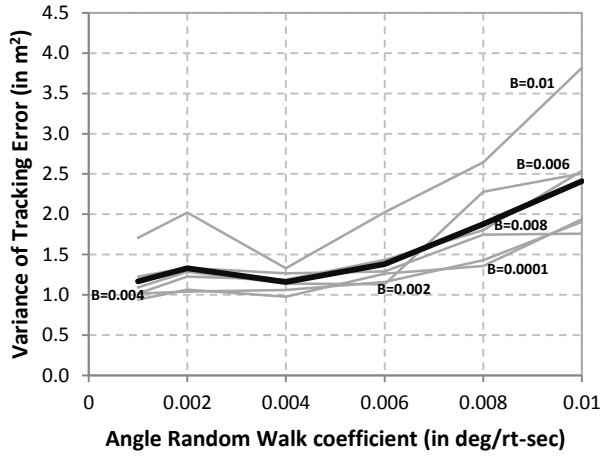

FIGURE 9: VARIANCE OF TRACKING ERROR WITH VARYING ANGLE RANDOM WALK COEFFICENTS

Figure 9 indicates that the variance in the tracking error changes significantly as the angle random walk coefficient is varied from its minimum to maximum value. The variance is representative of the precision with which the vehicle is tracked. Specifically, the variance of tracking error increases by about 150% as the angle random walk coefficient increases from 0.001 to 0.01 $°/\sqrt{s}$. Further, the variation in vehicle tracking precision with angle random walk coefficient also appears to be roughly linear in nature, within the range of values under consideration.

Effects of Bias Instability on Vehicle Tracking Accuracy and Precision

A similar analysis as performed for angle random walk noise is performed for bias instability. In this case, the relationship between vehicle tracking precision and bias instability coefficients is less apparent. The bias instability coefficients are varied from $0.0001°/sec$ to $0.01°/sec$. The angle random walk coefficients have the units $°/\sqrt{s}$. Figure 10 includes the mean tracking error values as bias instability increases, for various fixed values of angle random walk coefficients. As before, the thick line indicates the mean tracking error averaged over the various fixed values of the angle random walk coefficients. The plot indicates that the mean tracking error increases moderately, i.e. the vehicle tracking accuracy decreases, as the bias instability noise component in the inertial sensor increases. Further, this relationship is approximately linear in nature within the range under consideration. The plot also indicates that the mean accuracy of tactical-grade sensors is slightly better than other commercial-grade or MEMS sensors, when considering vehicle tracking applications.

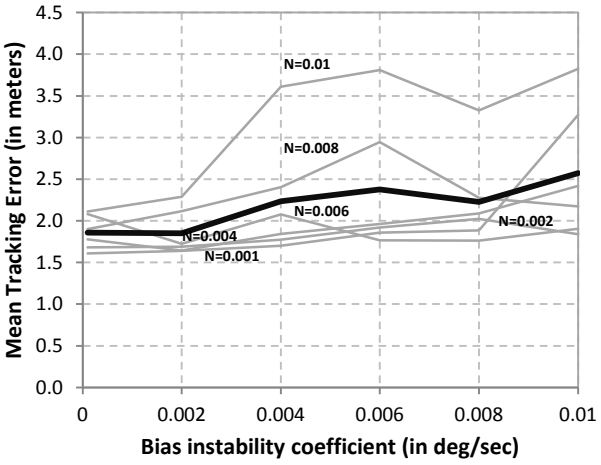

FIGURE 10: MEAN TRACKING ERROR FOR VARYING BIAS INSTABILITY COEFFICIENTS

Figure 11 depicts the precision in tracking error, and indicates that the variance in tracking error increases moderately as bias instability in the sensor increases. This implies that sensors with higher bias instability coefficients have a poorer precision. Further, the simulations indicate that tactical-grade sensors, which have a bias instability of the order of $0.0001°/sec$, yield a marginally higher precision in vehicle tracking as compared to simulated low-cost MEMS inertial sensors, which have a bias instability of the order of $0.01°/sec$. The pertinent issue now is to examine if the apparent advantages offered by increased precision of tactical-grade sensors, as observed from the simulations for both angle random walk and bias instability coefficients, justify the cost of these sensors. The next section discusses this issue by simulating some of the available sensors and comparing their accuracy and precision with their approximate purchase cost.

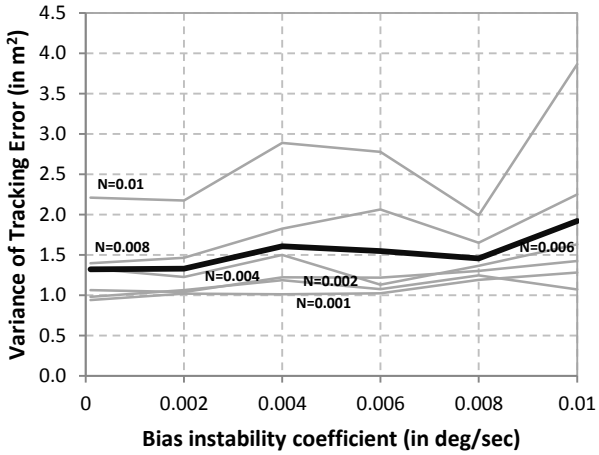

FIGURE 11: VARIANCE OF TRACKING ERROR WITH VARYING BIAS INSTABILITY COEFFICIENTS

COMPARISON OF VEHICLE TRACKING PERFORMANCE USING AVAILABLE INERTIAL SENSORS

This section presents a cost versus performance simulation-based analysis of some of the inertial sensors available in the market today. From the viewpoint of a systems engineer who is trying to select the appropriate inertial sensor for a particular application and within budgetary constraints, it only seems natural to have a cost-benefit analysis close at hand. Specifically, it is advantageous to know the cost of obtaining a desired level of accuracy and precision in vehicle tracking, even if it is not one of the primary design constraints. A few inertial sensors which were representative of their 'cost' category were selected for simulation. These sensors along with their characteristics are listed in Table 3.

Figure 12 includes the approximate price of the selected sensor plotted against the mean tracking error delivered by a simulated sensor with the same characteristics. The thick line indicates the mean tracking error achieved during vehicle tracking with the specific simulated sensor. The thin lines represent one standard deviation from the mean value, as obtained from multiple simulations. In the sensor selection process, the plot may be used as an indicator of the cost of achieving a pre-specified accuracy. Alternatively, in the sensor design process, it may be used as an indicator of the possible

accuracy achieved when constrained by a pre-specified cost. From Figure 12 it may be observed that the sensors may be broadly grouped into two 'cost' categories, the low-cost category and the higher-end category. Specifically, the plot indicates that the mean tracking error for low-cost sensors, i.e. sensors which cost less than USD 2000, is over 1 m. On the other hand, the mean tracking error for inertial sensors in the higher-end category, which cost USD 2000 or above, is less than 1 m. Further, for sensors in the higher-end category, the mean tracking error is relatively constant and appears to be independent of cost.

TABLE 3: SELECTED AVAILABLE SENSORS

Sensor	**Angle random walk coefficient,** $N\ (^\circ/\sqrt{sec})$	**Bias instability coefficient,** $B\ (^\circ/sec)$
Analog Devices ADIS16367 [22]	0.033	0.013
Gladiator Technologies Landmark 10 [23]	0.014	0.007
Gladiator Technologies Landmark 30 [24]	0.01	0.003
Honeywell HG1700 [21]	0.0016	0.0003

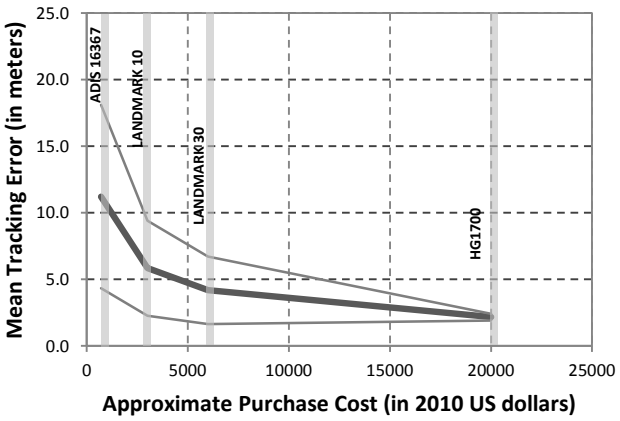

FIGURE 12: MEAN TRACKING ERROR VS. PRICE FOR SELECTED INERTIAL SENSORS

More importantly though, Figure 13 includes the approximate cost of the listed sensor plotted against the variance of tracking error obtained by a simulated sensor with the same characteristics. This plot is indicative of the vehicle tracking precision delivered by the inertial sensor as a function of cost. It is observed that significant improvement is obtained as cost increases from the low-cost category to the higher end category. This is evident by observing the variance of tracking error of the ADIS16367 and Landmark 10 inertial sensors. However, the law of diminishing returns limits the improvement in vehicle tracking precision as cost increases further in the higher-end category. In other words, it requires more and more expensive inertial sensors in order to obtain higher precision. Specifically, as shown in Figure 13, the cost of the sensor can be approximated by a power law, where the variance of tracking error approaches zero asymptotically, as the cost of the sensor approaches infinity. This represents a fundamental limitation in the sensor selection and/or design process. The associated coefficient of correlation for the fitted curve is 0.995, indicating that the power law may indeed be a good functional approximation for the relation between sensor cost and vehicle tracking error precision. In Figure 13, the relationship is described as follows:

$$\sigma^2 = A(Cost^{-B}) \qquad (7)$$

where σ^2 is the tracking error variance (in m^2), A = 508.4, B = 0.586, and sensor cost is in 2010 US dollars. It may be observed that the return on investment of inertial sensors for vehicle tracking purposes reduces as cost increases, since reasonable performance is offered by even cheaper sensors in the higher-end category, such as the Landmark 10. However, the cost-to-performance ratio metric is application specific, and for several applications, such as autonomous vehicles requiring high-gain feedback, the higher cost may be justified in order to achieve higher precision.

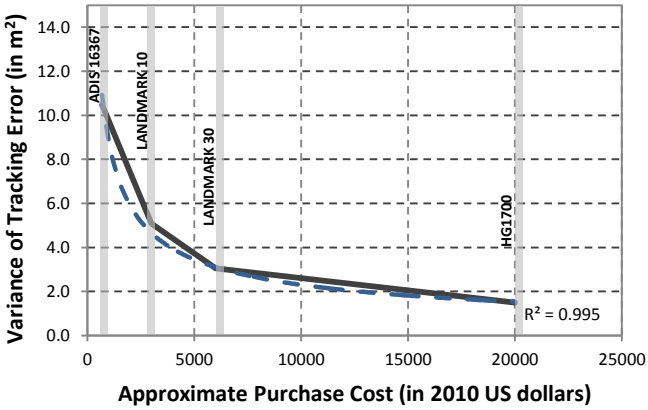

FIGURE 13: VARIANCE OF TRACKING ERROR VS. PRICE OF SELECTED INERTIAL SENSORS

CONCLUSIONS

From the above simulations and analysis, it can be concluded that the terrain-based algorithm can be used for vehicle tracking even with low-cost sensors. Additionally, an analysis of the effects of inertial sensor characteristics on vehicle tracking error reveals that the mean tracking error increases as the values of the noise-characterizing coefficients increase. Consequently, it is observed that tactical-grade sensors tend to provide higher precision than their low-cost MEMS counterparts, which is as expected. It is also observed that that the relationship of the vehicle tracking precision with the angle random walk coefficient is approximately quadratic in nature, and with bias instability coefficient is approximately linear in nature, within the range in consideration. Further, the

angle random walk and bias instability coefficients appear to be linearly related to vehicle tracking precision.

Further, the cost versus accuracy and cost versus precision plots indicate that as cost increases the vehicle tracking performance increases significantly at first, but as the cost increases further, the improvement in tracking performance is marginal. Specifically, it requires more expensive sensors to achieve the same scale of improvement in vehicle tracking precision in the higher-end category of sensors.

ACKNOWLEDGMENTS

This work was performed with the help of funding provided by the Federal Highway Administration under the Exploratory Advanced Research Program (FHWA BAA DTFH61-09-R-00004). This project is being performed in collaboration with Dr. David Bevly at the Auburn University.

REFERENCES

[1] F. Gustafsson, et al., "Particle filters for posiitoning, navigation and tracking," *IEEE Transactions on Signal Processing*, vol. 50, no. 2, 2002.

[2] A. J. Dean, "Terrain-based Vehicle Localization using Attitude Measurements," Ph.D. Thesis, The Pennsylvania State University, 2008.

[3] A. Dean, R. Martini, and S. Brennan, "Terrain-Based Road Vehicle Localization using Particle Filters," in *Proceedings of the 2008 American Control Conference*, 2008, pp. 236-241.

[4] S. Williams, G. Dissanayake, and H. Durrant-Whyte, "Towards terrain-aided navigation for underwater robotics," *Advanced Robotics*, vol. 15, no. 5, pp. 533-549, 2001.

[5] N. Vandapel, R. R. Donamukkala, and M. Hebert, "Unmanned Ground Vehicle Navigation Using Aerial Ladar Data," *The International Journal of Robotics Research*, vol. 25, no. 1, pp. 31-51, 2006.

[6] T. Tsumura, H. Okubo, and N. Komatsu, "A 3-D position and attitude measurement system using laser scanneds and corner cubes," in *Proceedings of the 1993 IEEE International Conference on Intelligent Robots and Systems*, Yokohoma, Japan, 1993, pp. 604-611.

[7] R. Talluri and J. K. Aggarwal, "Position Estimation for an autonomous mobile robot in an outdoor environment," *IEEE Transactions on Robotics and Automation*, vol. 8, no. 5, pp. 573-584, 1992.

[8] V. Gupta and S. Brennan, "Terrain-based vehicle orientation and estimation combining vision and inertial measurements," *Journal of Field Robotics*, vol. 25, no. 3, pp. 181-202, 2008.

[9] J. Vaganay and M. J. Aldon, "Attitude estimation for a vehicle using inertial sensors," *Control Engineering Practice*, vol. 2, no. 2, pp. 281-287, 1994.

[10] N. Barbour and G. Schmidt, "Inertial Sensor Technology Trends," *IEEE Sensors Journal*, vol. 1, no. 4, pp. 332-339, 2001.

[11] N. Yazdi, F. Ayazi, and K. Najafi, "Micromachined Inertial Sensors," in *Proceedings of the IEEE*, vol. 86, 1998, pp. 1640-1659.

[12] N. El-Sheimy, H. Hou, and X. Niu, "Analysis and Modeling of Inertial Sensors Using Allan Variance," *IEEE Transactions on Instrumentation and Measurement*, vol. 57, no. 1, pp. 140-149, 2008.

[13] L. C. Ng and D. J. Pines, "Characterization of Ring Laser Gyro Performance using the Allan Variance Method," *Journal of Guidance*, vol. 20, no. 1, 1996.

[14] D. M. Bevly, "Global Positioning System (GPS): A Low-Cost Vehicle Sensor for Correcting Inertial Sensor Errors on Ground Vehicles," *Journal of Dynamical Systems, Measurement and Control*, vol. 126, no. 2, pp. 255-264, 2004.

[15] S. Godha and M. E. Cannon, "Integration of DGPS with a Low Cost MEMS - Based Inertial Measurement Unit (IMU) for Land Vehicle Navigation Application," in *Proceedings of the ION GPS '05*, Long Beach, CA, USA, 2005.

[16] "IEEE Standard Specification Format Guide and Test Procedure for Single-Axis Interferometric Fiber Optic Gyros," IEEE Std. 952-1997, 1998.

[17] A. Gelb, J. F. Kasper, R. A. Nash, C. F. Price, and A. A. Sutherlan, *Applied Optimal Estimation*, A. Gelb, Ed. 1974.

[18] D. W. Allan, "Statistics of Atomic Frequency Standards," *Proceedings of the IEEE*, vol. 54, no. 2, pp. 221-230, 1966.

[19] J. Wall and D. Bevly, "Characterization of Inertial Sensor Measurements for Navigation Performance Analysis," in *Proceedings of the ION GNSS*, 2006, pp. 2678-2685.

[20] A. J. Dean, J. Langelaan, and S. N. Brennan, "Initializing an Unscented Kalman Filter using a Particle Filter," in *Proceedings of the Dynamic Systems and Control Conference*, 2009.

[21] HG 1700 Datasheet. (2011, Mar.) Honeywell International website. [Online]. http://www.honeywell.com

[22] Analog Devices ADIS16367 Datasheet. (2011, Mar.) Analog Devices website. [Online]. http://www.analog.com

[23] Landmark 10 Datasheet. (2011, Mar.) Gladiator Technolgies website. [Online]. http://www.gladiatortechnologies.com

[24] Landmark 30 Datasheet. (2011, Mar.) Gladiator Technologies website. [Online]. http://gladiatortechnologies.com